Journal of Sound and Vibration 330 (2011) 636–651

Contents lists available at ScienceDirect

Journal of Sound and Vibration

journal homepage: www.elsevier.com/locate/jsvi

# A numerical study on stick–slip motion of a brake pad in steady sliding

J. Behrendt *, C. Weiss, N.P. Hoffmann

*Hamburg University of Technology, Institute of Mechanics and Ocean Engineering, Eißendorfer Straße 42, 21073 Hamburg, Germany*

ARTICLE INFO

*Article history:*
Received 17 November 2009
Received in revised form
22 June 2010
Accepted 23 August 2010
Handling Editor: M.P. Cartmell
Available online 8 October 2010

ABSTRACT

A numerical model for an elastic brake pad sliding under constant load and with constant velocity over a rigid surface is investigated by finite element analysis. The geometry is taken to be two-dimensional, the contact is assumed to follow the laws of continuum mechanics and temporal and spatial resolution are such that dynamical effects localized at the interface are resolved. It turns out that at the contact interface localized slip events occur either in the form of long-lasting slip pulses, or in the form of brief local relaxations. Macroscopically steady sliding, macroscopic stick–slip motion or slip–separation dynamics occurs, depending on the macroscopic relative velocity. While structural oscillations of the brake pad do not seem to play a significant role during steady sliding at least one structural oscillation mode becomes synchronized with the interfacial dynamics during stick–slip or slip–separation motion. Assuming a given friction law for the interface, the macroscopically observed friction coefficient depends considerably on the underlying dynamics on the interface.



## 1. Introduction

Friction brakes are widely used. Unfortunately, quite often unwanted noise and vibration problems arise in such systems [1,2]. Although considerable knowledge on underlying mechanisms, interaction chains and influence factors, etc. has become available, substantial discrepancies between predictions and observations do still exist. One of the reasons for the presently still unsatisfying situation is often hypothesized to be the poor understanding of the true dynamic processes taking place at the friction interface. Basic mechanisms are outlined in [3,4]. In fact much knowledge on friction-induced vibration has been obtained on the basis of macroscopic rigid-body models with point contacts [5]. But also on spatially extended contact of compliant bodies a large body of fundamental work is available now [6]. Wave-propagation [7,8] or pulse and front dynamics [9,10] is thought to play a role at the friction interface in a microscopic sense. The relation between the macroscopic dynamics and the microscopic processes at the friction interface itself seems to be rather poorly understood. Only comparatively few studies seem to have been conducted [11,12]. Especially the interaction between interfacial wave- or pulse-processes and system vibration effects is still to a large extent a matter of hypotheses.

The present work therefore attempts to gather some additional understanding on the interrelation between micro-dynamics, i.e. dynamical phenomena localized at the friction interface (like slip pulses), and macro-dynamics, which is in the following understood as the dynamics on typical engineering length- and time-scales. For simplicity the whole analysis has been focused on a very simple model system of a steadily sliding brake pad. Note that in this context the macroscopical behavior is described by the forces and motions of the contact points where the subsystem 'brake' is connected to the main

* Corresponding author.
*E-mail address:* jasper.behrendt@tu-harburg.de (J. Behrendt).

0022-460X/$ - see front matter © 2010 Elsevier Ltd. All rights reserved.
doi:10.1016/j.jsv.2010.08.030

system. The study has strongly been driven by the question to what extent the microscopic processes at the friction interface can be covered in a pure macro-analysis through the use of an appropriate contact and friction model.

The paper is structured as follows: first the geometric and material models are described and the numerical solution process is outlined. The subsequent results section presents the findings; for a reference configuration the macroscopic sliding velocity turns out as a parameter separating a number of different regimes of resulting dynamics. Some qualitative explanations for the observed behavior are given. Subsequently the results of a number of design variations are presented and a summarizing discussion concludes the paper.

## 2. Modeling and analysis approach

Based upon the actual size of a brake pad used in a wind-energy plant, a rectangular block of friction material of dimensions $70 \times 35 \times 10$ mm is considered. Contact with a rigid countersurface moving with constant velocity $v$ is assumed on a surface area of 70 mm $\times$ 35 mm. The 'back-side' of the pad is taken to be rigid and free only to move in a direction normal to the friction interface. This was achieved by kinematically coupling the nodes of the 'back-side' of the pad to a central coupling point (see Fig. 1). The coupling point is constrained by boundary conditions, allowing only displacements in the *Y*-direction. A constant normal loading of 245 N is imposed, which corresponds to the nominal normal stress of 0.1 MPa at the contact interface, which again is a typical value from the actual application. The point force of 245 N is acting on the coupling point. Because of the kinematic coupling the load is evenly distributed to the friction interface. Even though it is a two-dimensional analysis a transverse dimension of the pad is given, because it has an influence on the value of normal stress at the contact interface and the general stress state caused by the point load of 245 N. A state of plane strain is assumed as the transverse dimension of the pad is of the same order of magnitude as the other dimensions. With respect to the material, the pad is modeled as homogeneous, isotropic and elastic. For numerical purposes (mainly to avoid ringing and the collapse of an element during a time-step using an explicit solver) some numerical damping usually in the form of bulk viscosity has to be postulated. The bulk viscosity has been set to comparatively high values in order to achieve a good numerical efficiency and mimick at least some material damping. The bulk viscosity causes a pressure $p$ that counteracts the temporal change of the volume $\dot{\varepsilon}_{\mathrm{vol}}$ of an element (see Eq. (1)):

$$p = b_1 \rho c_d L_e \dot{\varepsilon}_{\mathrm{vol}}, \tag{1}$$

where $c_d$ is the longitudinal wave speed, $L_e$ the characteristic element length, $\rho$ the density and $b_1$ a parameter that is set to 0.72. Of course this is a crucial assumption, since the high sensitivity of friction-induced vibration with respect to specifics of damping is well known [16]. Definitely improved damping models will have to be studied in the future. Another severe simplification consists in the restriction to two-dimensional dynamics; all displacements are assumed to be within a plane defined by the direction of relative motion and the direction normal to the friction interface. In addition, the displacements are required to be homogeneous in the lateral direction. These assumptions do obviously constrain the dynamics at the interface considerably, e.g. oblique slip fronts are excluded, but also the influence of the side-faces cannot be evaluated. However, restricting the displacement dynamics to two dimensions, and thus reducing the numerical effort, does enable a first fundamental study and should be understood as a first step to a full three-dimensional picture.

The normal contact constraint is enforced with a Lagrange multiplier representing the contact pressure in a mixed formulation. This model represents a contact interface with an infinite contact stiffness (no 'overclosure' or intersection of the bodies), so the contact interface does not add any elastic components to the system. A detailed description of the method of Lagrange multiplier in contact dynamics can, e.g. be found in [13,14]. For friction a simple static, but velocity-dependent model is used, which is algebraically given as

$$\mu(v) = \mu_c + (\mu_s - \mu_c) \cdot \mathrm{e}^{-d_c \cdot v}. \tag{2}$$

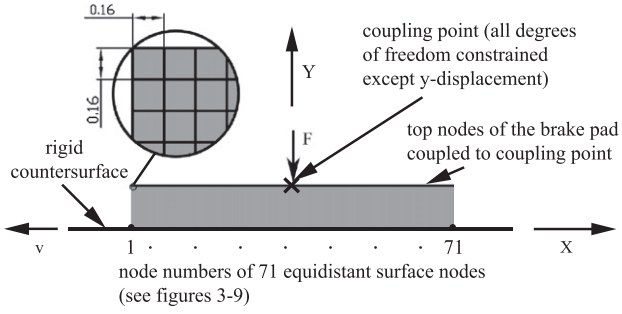


**Fig. 1.** Geometry of the model.

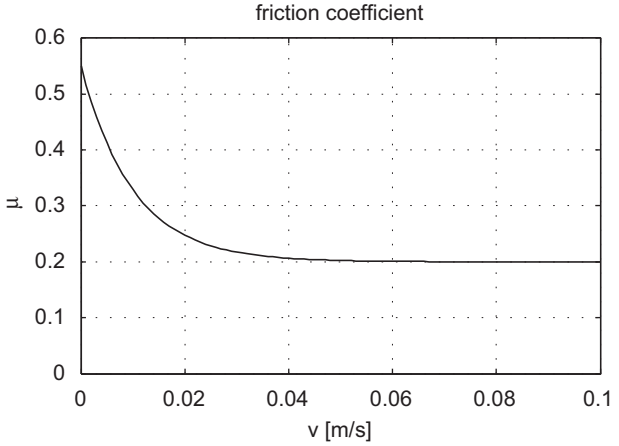


**Fig. 2.** Velocity-dependent friction coefficient.

**Table 1**
Computation steps.

| Step: | 1. Initial | 2. Force appl. | 3. Acceleration | 4. Results |
|---|---|---|---|---|
| Bound. c. | Application | Applied | Applied | Applied |
| Point force | 0 | Application | Applied | Applied |
| Velocity | 0 | 0 | Application | Applied |

From measurements based on the underlying application the coefficients have been determined to $\mu_s = 0.55$, $\mu_c = 0.20$, $d_c = 100\,\mathrm{sm}^{-1}$. Fig. 2 shows the characteristic. One should note that this friction model will in the following be used as the true friction model at the interface. Of course this is strictly speaking not correct, since the measured values are the macroscopically determined friction coefficients, not the true interfacial ones; nevertheless, to gain some first understanding of the relationship between micro- and macro-quantities throughout the study the given friction law will be used on the interfacial micro-scale. An imaginable rescaling for, or even identification of the actual microscopic friction from the measured macroscopic friction and dynamic system state is presently left as a future task.

The geometry of the model is discretized using finite elements. For the discretization the size of the elements, especially at the contact zone, has been chosen such that a further refinement of the mesh no longer changes the results in any substantial way. For that purpose a large number of test calculations have been conducted that have shown that at the contact zone nodal distances of about 0.16 mm are sufficient to resolve the appearing slip events to be described later. The pad was discretized with a regular mesh using $420 \times 60$ quadratic four-node bilinear elements (large strain) of the size $0.16\,\mathrm{mm} \times 0.16\,\mathrm{mm}$ (see Fig. 1). A reduced order integration with hourglass control mechanism has been used in order to keep the calculation time low. The model is then subjected to explicit time-integrations. The resulting time-steps are short enough ($10^{-7} \ldots 10^{-8}$ s) to ensure the stability of the explicit time discretization scheme. The short time steps guarantee that frequencies up to 550 kHz are resolved (assuming about 10 time-steps per period of a stipulated periodic process). The calculation is done in four steps (see Table 1):

1. Initial step: the boundary conditions (constraints of the coupling point and the rigid countersurface are applied) and the contact are established.
2. Force application step: the point force is applied to the coupling point.
3. Acceleration step: the rigid countersurface is accelerated to the velocity $v$.
4. Result step: the applied force and velocity are kept constant and the results are recorded.

The point force and the velocity are applied as a smooth time dependent s-shaped function in order to avoid numerical problems due to discontinuities. In the last simulation step the results presented in the following chapters are recorded. The displacements and velocities of 71 equidistant nodes of the friction surface are recorded and analyzed. To define the contact state of each node the following criteria are used:

- sticking: $|v_{\mathrm{node}} - v_{\mathrm{countersurface}}| \leq \varepsilon$ and $y_{\mathrm{node}} < \zeta$;
- sliding: $|v_{\mathrm{node}} - v_{\mathrm{countersurface}}| \geq \varepsilon$ and $y_{\mathrm{node}} < \zeta$;
- separation: $y_{\mathrm{node}} \geq \zeta$.

where $\varepsilon$ and $\zeta$ are set to $10^{-13}$ m/s and $10^{-13}$ m, respectively, to take round-off errors into account. After the final relative velocity has been reached, enough time is given to the computations to reach a steady state (or at least a quasi-steady state, if at all possible). Depending on the type of resulting motion, each calculation requires up to a day of computation time on a presently typical workstation with eight processor kernels. One should note that in the following only the resulting time-asymptotic solutions will be presented. Questions with respect to the very initial phases of macroscopic break-away, as well as questions with respect to transitional aspects, although of quite some relevance for applications, are left for future studies.

### 2.1. Modal analysis

The eigenmodes of the pads are computed using a setup almost identical to the one used in the above described time domain simulations. The mesh, the point force and the coupling to the coupling points remain identical. In difference to the time domain calculation the rigid countersurface does not move and because the modal analysis is not about determining the stability of the eigenmodes (complex eigenvalue analysis) the friction is neglected. The modal analysis is calculated stepwise with step one and two being identical to the time domain analysis. In the third step the modal analysis is performed. As the modal analysis is a linear analysis the nodes in contact with the countersurface remain fixed on it. As shown in the following chapters the eigenmodes of the pad have a dominating impact on the resulting dynamics. So the question comes up what a flexible countersurface (like a brake disc) would contribute to the resulting dynamics. Using a flexible pad and brake disc (or even a whole brake system) should result in far more complex eigenmodes. The friction interface dynamics is also expected to be much more complicated, because of the fact that both the brake pad and the brake disc have interacting interface dynamics. To see which part of the brake system has the greatest impact (and therefore is the most promising part to modify) on the involved eigenmodes the modal assurance criterium (MAC) is often used [15]. It is basically a correlation method, which compares the eigenmodes of each parts with the eigenmodes of the whole assembled system.

## 3. Results for a reference configuration

The present work has been motivated by a brake pad used in a wind-energy power-plant. Therefore, at first results based on the material properties as determined for this specific application are going to be presented. Some additional parameter studies with respect to material properties and geometric changes are presented subsequently. A widely used material for industrial plain bearings is polyamid (PA6 or PA66). Based on material characterizations Young's modulus of $E=1000$ MPa, a Poisson's ratio of $\nu=0.39$ and a mass density of $\rho=1150$ kg/m have been used for an extensive case study. Since on-site observations of the application had indicated that the vibration and noise characteristics of the system seem to depend strongly on the relative sliding speed between pad and countersurface, the relative velocity $v$ was taken as the primary control parameter of the system and simulations for about 30 different velocities were run. For each calculation both the 'microscopic', i.e. highly resolved dynamics at the interface, as well as the 'macroscopic' averaged dynamics on the engineering scales have been determined and will be presented and discussed in the following.

### 3.1. The ultralow-velocity regime: $v<0.7$ mm/s

For extremely low sliding speeds, i.e. for sliding velocities clearly below about 1 mm/s, the calculations suggest aperiodic stick–slip motion on a macroscopic scale, i.e. now and then the overall shear in the pad is relaxed a bit. Since the spatial and temporal resolutions of the present model have, however, been chosen to resolve also the dynamic processes at the interface, it is possible to analyze, how the macroscopically observed relaxation event is realized by processes at the interface itself.

For that purpose Fig. 3 shows selected system properties as evaluated over time at the interface. Fig. 3a depicts the kinematic state of the contact zone over time; when a surface region sticks, it is marked dark blue (black in print), when it slides it is marked green (grey in print), and when separation occurs the marking is red (white in print). For visualization purposes the interface state is evaluated at 71 positions, where position 1 corresponds to the trailing, position 71 to the leading edge of the brake pad. It can be seen that the macroscopic sliding event is generated at the interface by a number of slip pulses traveling from the rear to the front end of the pad. The individual pulses travel along the interface with an almost constant velocity, which is intersonic in the sense that it is between the propagation velocity of bulk pressure and bulk shear waves.

To understand why most of the slip pulses start at the rear end, Fig. 3b shows the normal pressure distribution at the interface. At the rear end the contact pressure drops to zero, which corresponds to the separation of the pad at its very end, as could have been expected from comparison with other contact mechanics problems. A low contact pressure does, however, mean a low critical shear value for initiation of local sliding. This seems to be the reason for the rear contact area acting as sort of a source zone for slip pulses. As a consequence of the individual slip pulses crossing the interface zone, the

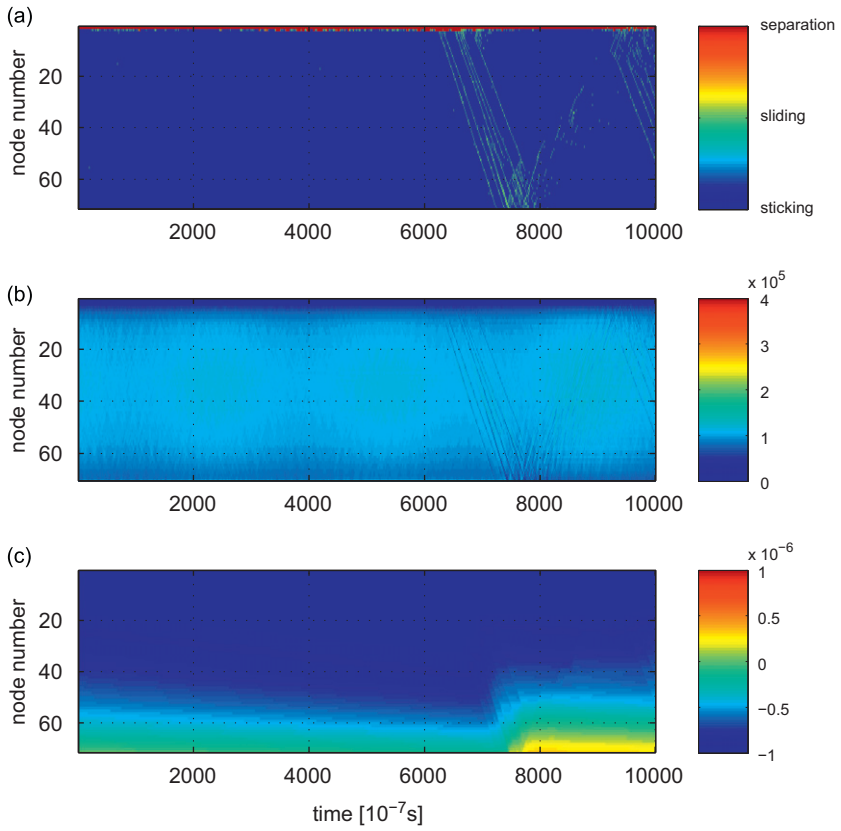


**Fig. 3.** Contact state (a), contact pressure (b) and pad surface displacement (c) along the pad over time for $v$=2.5 × 10$^{-4}$ m/s.

overall shear is reduced and the surface of the pad returns to a position corresponding to a state with a lower overall shear, see Fig. 3c representing the tangential displacement of the friction surface of the brake pad.

To summarize, for a very low sliding velocities the continuously increasing shear seems to relax aperiodically by the appearance of sort of a swarms of slip pulses crossing the interface from the rear to the front end of the brake pad. As shown later the transverse contraction of the material causes a force pulse acting orthogonal to the contact plane when the slip pulse travels through the contact plane. This force pulse excites eigenmodes of the pad, especially those with an eigenvector sensitive to forcing orthogonal to the contact plane. For, e.g. the slip pulse excites the first eigenmode at 3.35 kHz but the amplitude of the eigenmode is so small, that the contact pressure remains almost constant, so the reverse influence of the excited eigenmode on the slip pulse is minor; the damping dissipates the energy of the excited eigenmode almost completely before the following slip pulse feeds in some energy in the eigenmode again. In conclusion, the microscopic slip events do result in a macroscopic relaxation while keeping the overall load distribution and system dynamics largely unaffected. This changes when the relative velocity increases.

### 3.2. *Low-velocity stick–slip regime with synchronization to the first pad compression mode:* 0.7 mm/s < $v$ < 3.0 mm/s

When the relative velocity slightly exceeds values of about $v \approx 0.7$ mm/s the macroscopic motion is still largely generated by microscopic slip pulses; the slip phases do, however, become periodic in time and are correlated with a periodic oscillation of local and global contact pressure, see Fig. 4. Macroscopically the dynamics thus appears like a periodic build-up and relaxation of shear stress through a stick–slip type motion.

Apparently an interaction between the slip pulses and a structural vibration mode of the pad, namely the homogeneous vertical tension-compression mode, takes place. It seems plausible that structural vibrations of the bulk will – via the induced changes in contact pressure – have an influence on the generation and propagation of slip pulses. Conversely, a traveling slip pulse may also excite structural modes through its induced time-dependent deformation field. Qualitatively the interaction is clearly visible in Fig. 4, where the frequency at which the macroscopic slip events take place is remarkably close to the 3.35 kHz of the corresponding structural eigenfrequency.

When the relative velocity is increased to $v = 2.5$ mm/s the gross overall picture remains rather unchanged, Fig. 5. One may note, however, that the previously preferred propagation direction of the slip pulses is not that marked any more, and

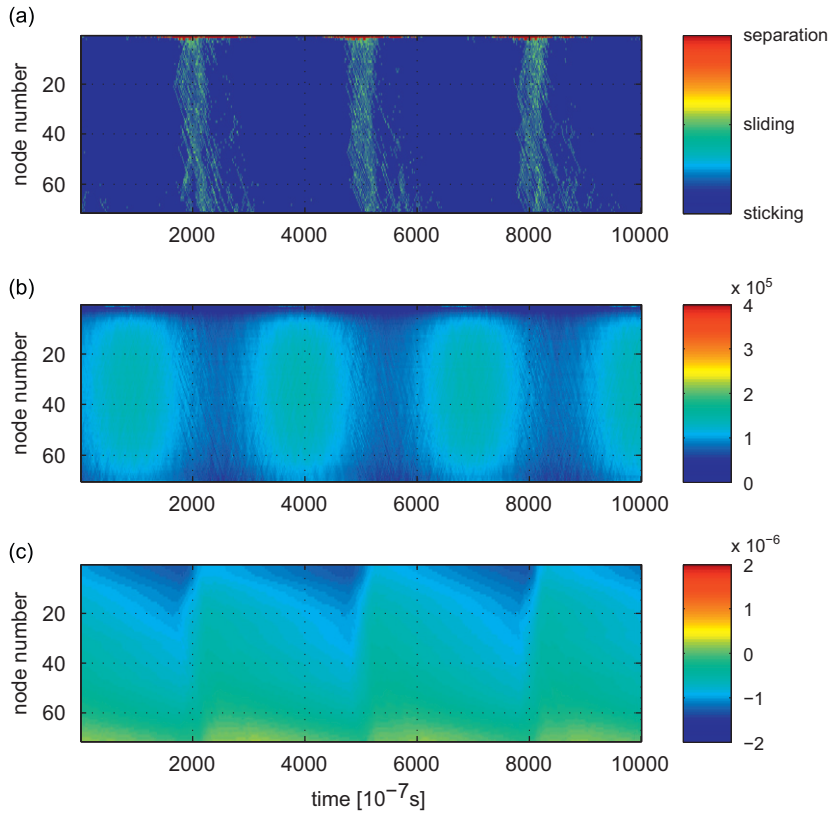


**Fig. 4.** Contact state (a), contact pressure (b) and pad surface displacement (c) along the pad over time for $v = 1.75 \times 10^{-3}$ m/s.

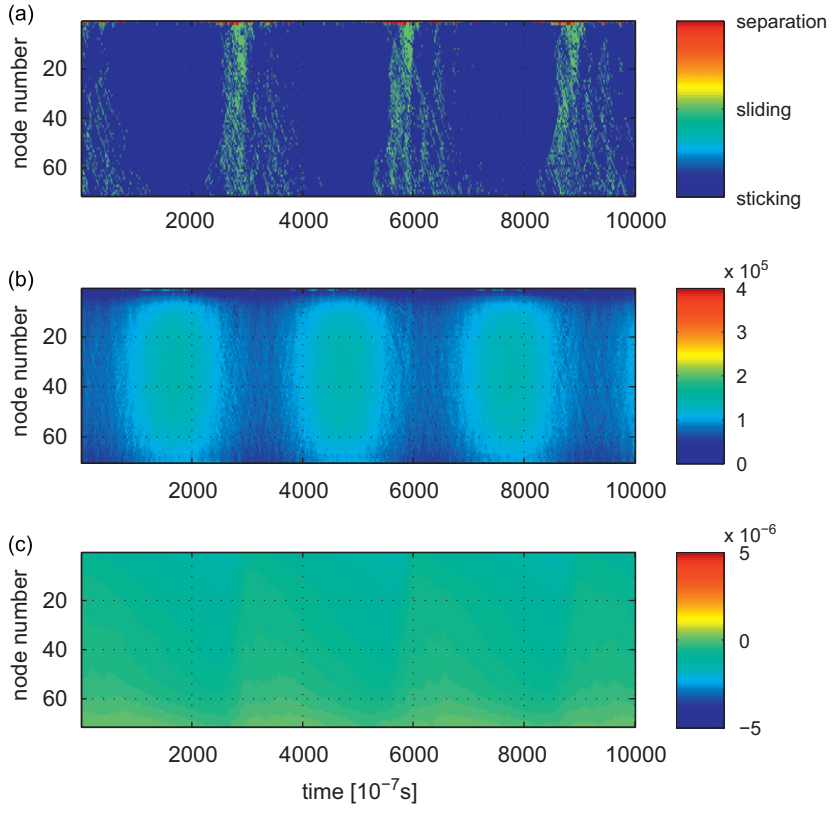


**Fig. 5.** Contact state (a), contact pressure (b) and pad surface displacement (c) along the pad over time for $v = 2.5 \times 10^{-3}$ m/s.

that some of the slip pulses look rather corrugated. A plausible explanation for this could be the larger amplitude of excited structural modes; the corresponding contact pressure oscillations seem to trigger local slipping now in a rather erratic fashion, and also the propagation of a single pulse should be hindered by the irregular contact pressure environment that it has to pass. Moreover it seems plausible that when a larger number of slip pulses are generated and terminated at different positions, the stress field at the interface will become quite complex, such that subsequent slip pulses will find an even more inhomogeneous background stress field in which they will try to propagate with more or less success.

The rather gradual changes towards more erratic slip-pulse behavior terminate in a transition to macroscopic steady sliding.

### 3.3. *Macroscopically steady sliding:* $3.0\,\mathrm{mm/s} < v < 10.0\,\mathrm{mm/s}$

When $v$ is increased further, the macroscopic stick–slip motion ceases and gives way to a sliding motion that appears steady on the macro-scale. Microscopically, slip is nevertheless still generated through relaxational slip pulses. In contrast to the response patterns for lower relative velocities, the pulses do now seem to be generated in a steady aperiodic fashion over time, which also corresponds to a mean contact pressure distribution that remains rather unchanged, see Fig. 6.

### 3.4. *High-velocity stick–slip regime with synchronization to a higher pad mode:* $10\,\mathrm{mm/s} < v < 80\,\mathrm{mm/s}$

Surprisingly, for further increased relative velocities another macroscopic stick–slip regime with dynamic participation of a structural mode can be observed, see Fig. 7.

The eigenfrequency of the mode, which is characterized by a time- and space-periodic modulation of contact pressure at the interface, is about 66.6 kHz. The macroscopic relaxation process reflects this frequency. On the friction interface itself again micro-scale slip events generate the relaxation, see Fig. 7a. At first sight of the contact state plot one could think again of the propagation of waves, this time from the front to the back of the pad. Closer inspection does, however, reveal that this impression is deceiving; the individual slip events come in the form of lasting pulses, sometimes only in the form of short-lived slipping; during a macro-slip phase the front areas of the pad do indeed start to slide earlier than the rear areas. This is, however, not caused or correlated to an individual slip pulse propagating, but originates in the lower contact pressure at the front end of the pad. The velocity of the macroscopic slip front thus is not just a simple footprint of the micro-scale events, but a more complicated feature that seems to be caused by the overall interaction of microscopic slip

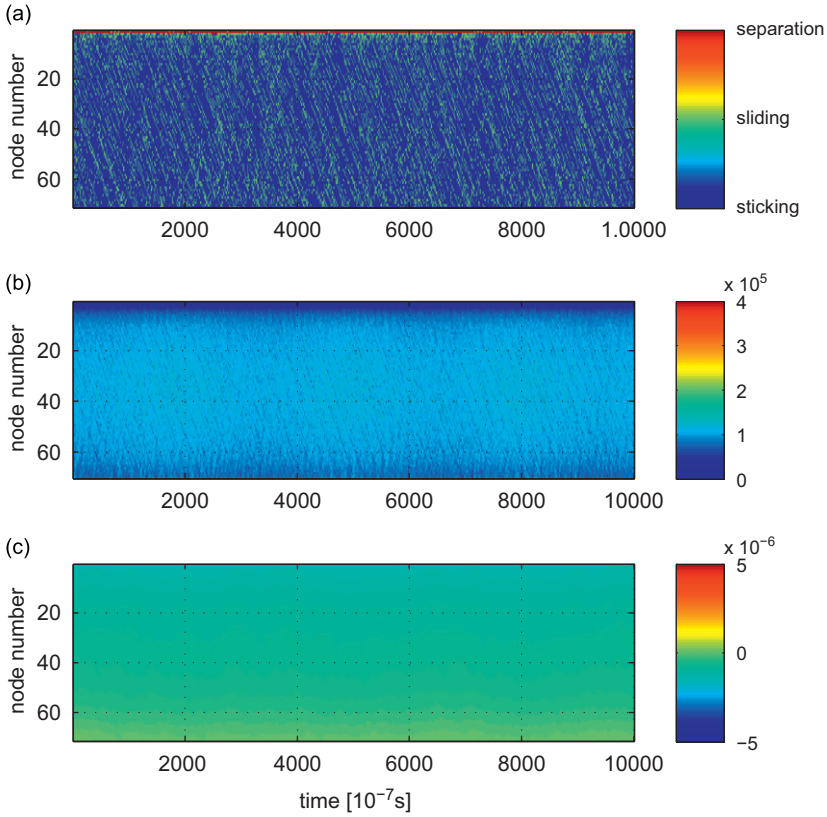


**Fig. 6.** Contact state (a), contact pressure (b) and pad surface displacement (c) along the pad over time for $v = 5.0 \times 10^{-3}\,\mathrm{m/s}$.

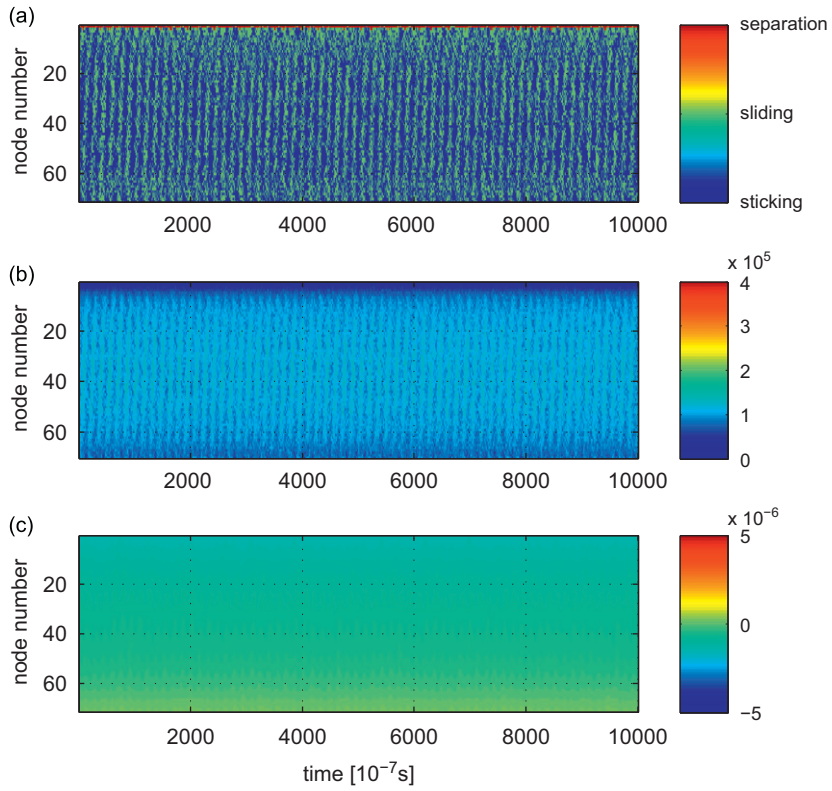


**Fig. 7.** Contact state (a), contact pressure (b) and pad surface displacement (c) along the pad over time for $v$=0.0125 m/s.

events, the macroscopic time-averaged pressure distribution and the macroscopic oscillation of contact pressure due to the excitation of the 66.6 kHz mode. The 'squeal' frequency of 66.6 kHz is much higher than the usual break squeal (1–16 kHz) and above the highest frequency that a human being can hear. Therefore this frequency range does not cause disturbing noises and is usually not explored. But there is no reason why stick-slip should not occur also in the ultrasonic regime.

### 3.5. *Stick–slip–separation regime:* $v > 40\,\mathrm{mm/s}$

For relative velocities beyond about 4 cm/s the motion of the pad at the interface starts to show separation events, see Fig. 8.

Before describing the corresponding dynamical state, one should note that the before-mentioned stick–slip regime coexists with the present stick–slip–separation regime for relative velocities between 4 and 8 cm/s. Increasing $v$ slowly, the stick–slip state remains stable up to 8 cm/s. Then the state abruptly undergoes a transition to a dynamics involving marked separation effects. Contrariwise, the stick–slip–separation dynamics can be followed towards lower $v$ down to about 4 cm/s; i.e. the transition between the states is hysteretic.

Close to the onset, the spatio-temporal contact state consists of a complex pattern of sticking, sliding and separation events, see Fig. 8a. Typically separation phases are adjacent to slip phases, which corresponds to earlier findings on slip–separation events. Surprisingly, within the pad length the dynamics does not show a homogeneous distribution, but different neighboring zones of stick–slip motion, stick–slip–separation motion and slip–separation motion do exist.

For even higher relative velocity $v$ the brake pad momentarily completely loses contact with the countersurface in a time-periodic fashion, see Fig. 9; sort of 'free-flight' phases are followed by phases in contact, which in itself are again characterized by stick–slip motion. Interestingly, the frequency of the lift-off and contact cycles at first corresponds closely to the elastic volume mode at about 3.35 kHz that had already previously been involved in one of the stick–slip motion regimes. The vibration state of the pad itself does, in addition, also show contributions from modes with higher frequency, as can most easily be seen from the displacement field evolution in Fig. 9b. For completeness it should be mentioned that a further increase in $v$ results in period doublings of the described jump-stick–slip motion. Since period doubling is, however, well known from vibro-impact systems, the corresponding findings are not discussed further here.

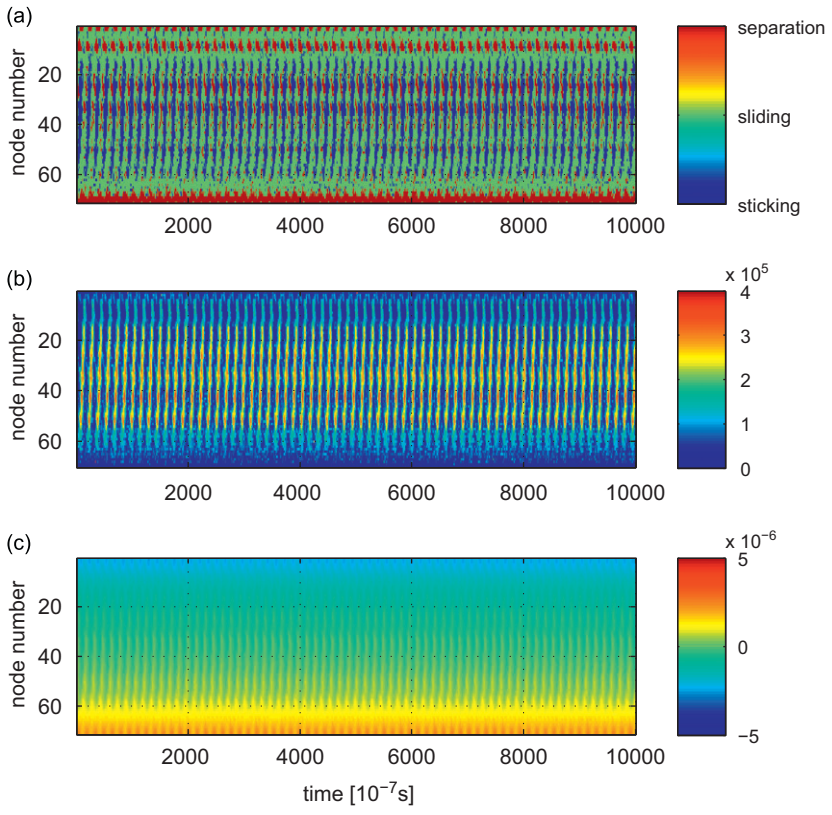


**Fig. 8.** Contact state (a), contact pressure (b) and pad surface displacement (c) along the pad over time for $v$=0.089 m/s.

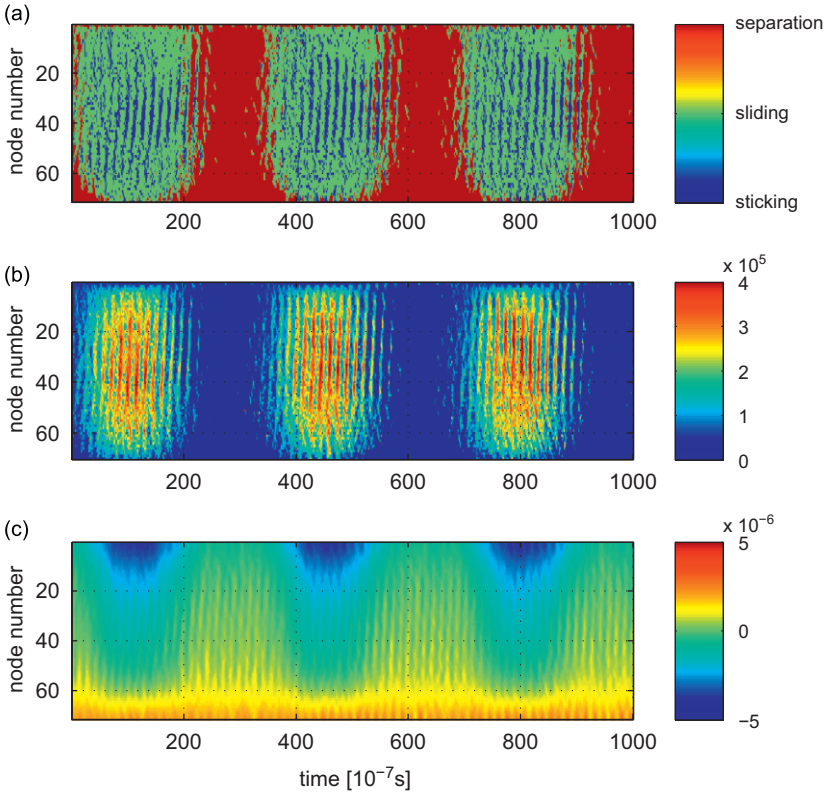


**Fig. 9.** Contact state (a), contact pressure (b) and pad surface displacement (c) along the pad over time for $v$=0.1 m/s.

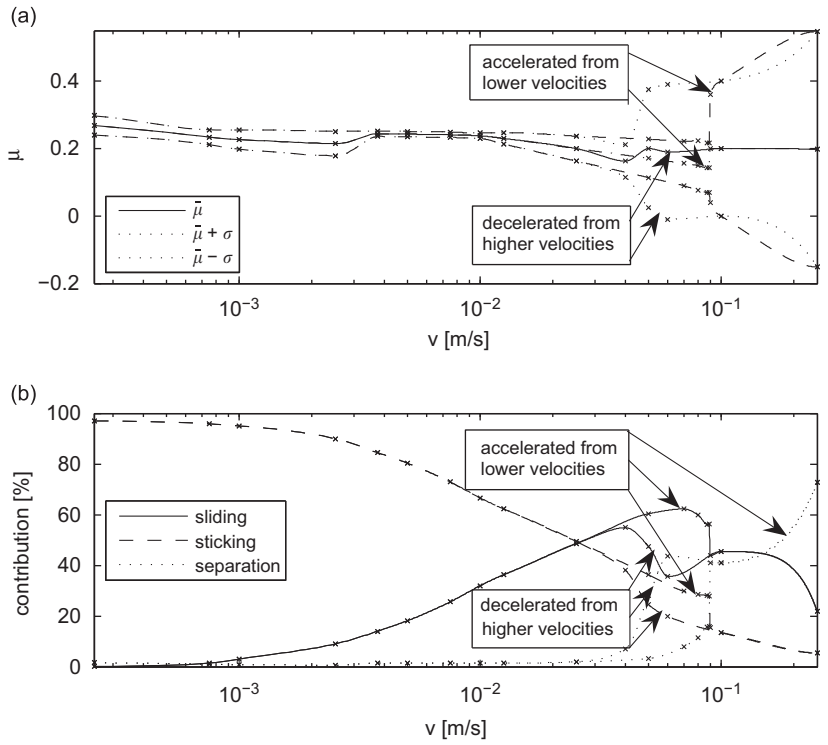


**Fig. 10.** $E = 1.0 \times 10^3$ MPa, $\nu = 0.39$. Effective macroscopic friction coefficient $\overline{\mu}_m$ and its standard deviation (a), temporal contributions of stick, slip, and separation (b), both vs. relative velocity $v$.

### 3.6. Apparent friction on the macro-scale

On the macroscopic length- and time-scales relevant for the functional design of the system, the numerous microscopic processes taking place at the interface will primarily be noticed in the form of an effective friction coefficient. Defining the momentary macroscopic friction coefficient $\mu_m(t)$ as the ratio of the momentary tangential reaction force to the constant normal load, one obtains a friction coefficient varying on the high-frequency time-scales of the interface processes. Averaging out the time-dependency, one may define an averaged macroscopic friction coefficient $\overline{\mu}_m(t)$, which finally is the relevant quantity for designing the friction brake as a system.

From the calculations discussed above the time-averaged macroscopic friction coefficient, and also a measure for the additional temporal fluctuations of the macroscopically observed friction force, can be evaluated. Fig. 10a shows the resulting macroscopic friction coefficients as a function of relative sliding velocity. Obviously the dynamic processes at the interface do strongly affect the macroscopically observed friction; interestingly, for all regimes the mean friction coefficient is never larger than about 0.27, which is a surprisingly low value when considering the underlying microscopic friction law. Nevertheless, there are also quite some level differences between the different regimes. In addition, during stick–slip motion there is of course a substantial fluctuation in the friction force over time, while during steady sliding the macroscopic friction force shows only minor fluctuations.

To understand a bit better, how the averaged friction comes about, Fig. 10b also shows time-averaged contributions of sticking, sliding, and separation for all the regimes. Remarkably, although the different regimes can be distinguished – as has been done above – quite easily, the distribution behavior of sticking, slipping and lift-of-times is rather smooth. With increasing relative velocity the stick-time decreases and the slip time increases monotonically, and finally separation comes into play. So, although this analysis does not seem to give too much insight into details, it does give some intuition on why the average macroscopic friction decays with $v$.

### 3.7. Some considerations on the interaction between interfacial slip events and macroscopic vibration

The above results have shown that macroscopic stick–slip dynamics seems always correlated with microscopic slip pulses or localized slip events and macroscopic vibration of the brake pad. Among the many structural modes that the pad actually has, only two specific modes do, however, seem to get in some sort of synchronization with the interfacial dynamics. Moreover, each mode seems to become activated in a certain range of relative velocities only. To gain at least some qualitative understanding, we propose the following two arguments. First, from considering the relaxational nature

of the interfacial slip pulses, a slip-pulse frequency may be identified. If the maximum bearable tangential displacement at the interface is $\Delta x$, and assuming complete relaxation, slipping should be expected at time intervals of $\Delta t = \Delta x/v$; i.e. relaxational slip should occur with a frequency of $f_{\text{slip}} = v/\Delta x$. The slip-pulse frequency thus increases linearly with the sliding velocity. It seems to be plausible that different structural modes (each having its fixed natural frequency) will therefore be excited depending on the relative sliding speed. Especially, assuming that the structural modes are excited by the time-dependent forces generated at the interface through the slip events, it seems plausible that for slip-pulse frequencies beyond the natural frequency of a mode, this mode will not be excited in a substantial manner any more. Performing some simple static analyses to determine $\Delta x$ as a function of $v$ shows that this argument reasonably explains the disappearance of the stick–slip motion combined with the 3.35 kHz structural oscillation when $v$ exceeds values of about 3 mm/s.

The above argument explains why stick–slip-motion (coupling between structural oscillation and interfacial slip pulses) might disappear beyond certain critical relative velocities; in the case of very weakly damped structural modes it could – due to an analogous argument of entering a resonance region – also explain, why an increase of $v$ may sometimes initiate stick–slip. But there is also an energy argument, that a certain relative velocity has to be reached to trigger a structural oscillation. The temporal energy loss of an excited mode, e.g. due to structural damping, will – at first order of consideration – not depend on the sliding velocity, but be proportional to the square of the vibrational amplitude only. The vibration energy gained per time, on the other hand side, e.g. due to strain accumulation or dynamic instability, will, in contrast, at first order always be proportional to $v$. So, to keep up an equilibrium amplitude of the structural vibration, a certain critical relative velocity will have to be reached — otherwise substantial vibration amplitudes cannot equilibrate. One has to admit that the argument is sort of hand-waving and that – for improvement – the details of the modal damping under the influence of the interfacial dynamics will have to be understood better. This work is, however, left for future studies.

## 4. Variants: changes in material properties and a geometry modification

To gain further understanding of the influence of material parameters and geometry, three variants were considered. First, an increased Young's modulus of the pad material is considered to see the influences of modified wave-propagation velocities and structural natural frequencies. Second, Poisson's ratio is set to zero to investigate the influence of transverse contraction at the interface due to slip pulses. Third, the geometry of the pad has been turned into a wedge like form to introduce dependencies of wave or pulse propagation parameters along the interface and to introduce inhomogeneity into the structural vibration mode shapes.

### 4.1. Increased Young's modulus: $E = 1.0 \times 10^4$ MPa

The results for an increased Young's modulus are very similar to the reference configuration, except for one novel finding. Fig. 11 gives an overview by presenting the resulting macroscopic friction coefficient.

Again, for very low $v$ macroscopically aperiodic stick–slip results. Then a stick–slip can be detected, which is characterized by the same structural mode shape as in the reference configuration, while the natural frequency has increased to 10.6 kHz due to the increase in Young's modulus. When $v$ is increased further, the important novelty of this parameter combination shows up; instead of a transition to steady sliding and subsequently to the second mode of stick–slip, a mixture of two stick–slip modes appears, i.e. in this stick–slip motion two structural modes seem to be strongly excited and synchronized by the interfacial slip events. This sort of nonlinearly coupled mixed stick–slip mode seems to exist for relative velocities between 1 and 3 mm/s, thus forming a transition between the neighboring pure stick–slip modes.

From the findings one may conclude that overlapping stick–slip regimes may lead to macroscopically mixed stick–slip, which means that more than one structural mode is excited. Thinking about the interaction mechanisms between the interfacial slip events and the macroscopic structural oscillations, this does indeed not seem to be implausible and might correspond to a weak coupling that structural oscillations should have due to their joint excitation through interfacial slip pulses or slip events.

### 4.2. Vanishing Poisson's ratio: $E = 1.0 \times 10^3$ MPa, $\nu = 0$

Since slip pulses are primarily dominated by displacements in directions in the plane of the contact surface, excitation of the structural modes due to forces normal to the contact surface might be conjectured to originate primarily as a consequence of lateral contraction effects. Setting down Poisson's ratio in the computation to zero does support this hypothesis, see Fig. 12.

Up to velocities of $v = 1$ cm/s macroscopically steady sliding results. Then a macroscopic stick–slip like behavior is observed, which is accompanied by a pad structural oscillation that is best characterized by an oscillatory contact pressure oscillation with one nodal line at half the length of the pad, i.e. the contact pressure increases in the front part of the pad

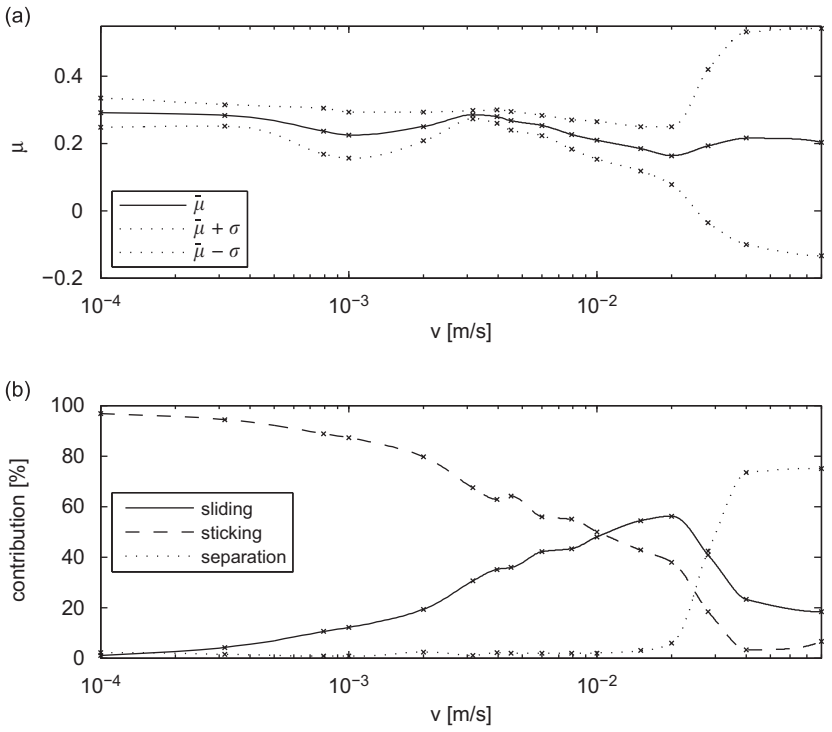


**Fig. 11.** $E = 1.0 \times 10^4$ MPa, $\nu = 0.39$. Effective macroscopic friction coefficient $\overline{\mu}_m$ and its standard deviation (a), temporal contributions of stick, slip, and separation (b), both vs. relative velocity $v$.

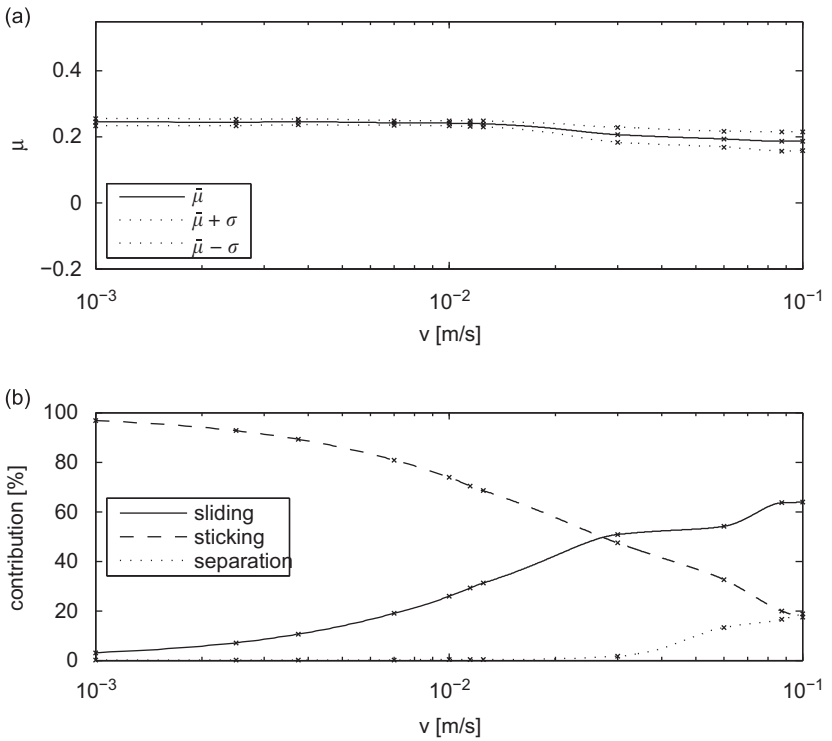


**Fig. 12.** $E = 1.0 \times 10^3$ MPa, $\nu = 0$. Effective macroscopic friction coefficient $\overline{\mu}_m$ and its standard deviation (a), temporal contributions of stick, slip, and separation (b), both vs. relative velocity $v$.

when it decreases at the rear part, and vice versa. This stick–slip motion then, for sliding velocities beyond about $v=7$ cm/s, again transforms into stick–slip–separation behavior very similar to the one described already previously.

### 4.3. Wedge like geometry of the brake pad

Most calculations based on the block-like geometry of the brake pad have shown that slip pulses propagating across the contact interface and the form of structural mode shapes seem to play a crucial role in the appearance of macroscopic stick–slip motion. One could suspect that both aspects should be strongly affected by the specific geometry of the pad itself; a wedge like pad, see Fig. 13, has therefore been chosen as a simple, but still feasible, design alternative.

The results are indeed striking; for the relative velocities considered, the system does not show any marked macroscopic stick–slip, and also the stick–slip–separation dynamics seems to be much weaker than with the rectangular brake pad. From Fig. 14 one can see that the resulting macroscopic friction coefficient does still vary somewhat, and that also the temporal contributions of stick, slip and separation vary, but macroscopic stick–slip is absent as well as marked vibro-impact dynamics.

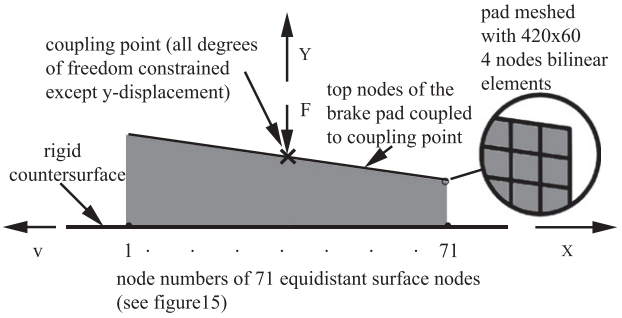


**Fig. 13.** Wedge like pad geometry.

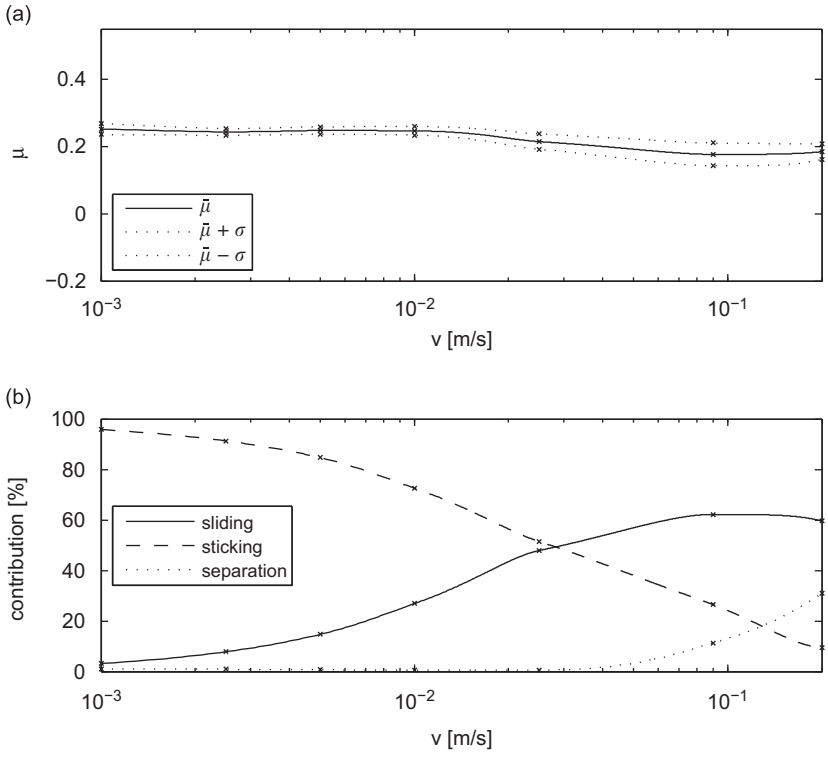


**Fig. 14.** Wedge like pad geometry, $E=1.0\times10^3$ MPa, $\nu=0.39$. Effective macroscopic friction coefficient $\overline{\mu}_m$ and its standard deviation (a), temporal contributions of stick, slip, and separation (b), both vs. relative velocity $v$.

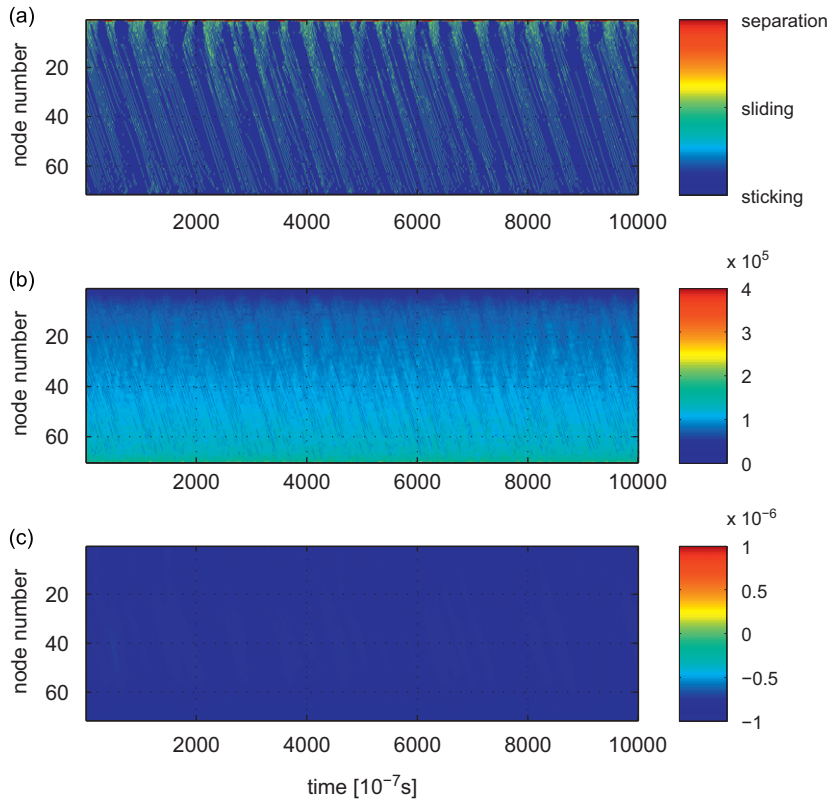


**Fig. 15.** Contact state (a), contact pressure (b) and pad surface displacement (c) along the pad over time for $v=5.0\times10^{-3}$ m/s and wedge like pad geometry.

Microscopically, see Fig. 15, the wedge like geometry seems to lead to erratic pulse propagation, which on the macro-scale basically appears as steady sliding with some noise in the friction force.

Two aspects seem to be responsible for the behavior: first, the overall static pressure distribution over the pad length is such that the local properties determining pulse generation and propagation do become more inhomogeneous than in the system with constant pad thickness. Second, the wedge like pad geometry strongly affects the overall dynamic contact pressure distribution due to the structural oscillation modes. The above dominantly observed mode with a rather homogeneous contact pressure oscillation has now been strongly suppressed and all modes show some variation in contact pressure oscillation along the pad. This seems to affect the interaction of pulse propagation and modal oscillation in a strongly inhibitive sense. In conclusion, the system with a wedge like geometry is characterized by irregular microscopic relaxations leading to regular steady macroscopic sliding, rather than the synchronized micro–macro stick–slip that had appeared before.

## 5. Summary, discussion and conclusions

To summarize, a generic model for sliding an elastic brake pad with constant velocity over a rigid surface has been set up. Only two-dimensional dynamics have been considered, i.e. displacements have been restrained to a plane orthogonal to the contact interface and parallel to the macroscopic motion direction. For the spatial discretization finite elements have been used and the discretization has been chosen such that also deformation events localized at the friction interface can be resolved. In general, to warrant a sufficiently fine discretization in space and time, extensive convergence studies have been performed to reach nodal distances and time-step sizes such that substantial changes in the results did not occur any more.

As a result, for the parameters given, sliding of the brake pad is always generated microscopically at the friction interface by slip pulses traveling along substantial distances along the brake pad, or by rather localized relaxations. The slip events may or may not excite structural vibration modes of the brake pad, depending on properties of the slip events themselves, or on the natural frequencies and the mode shapes of the vibration modes. When structural vibrations are not excited to substantial amplitudes, on the macro-scale the dynamics appears as steady sliding with some remaining stochastic component in the friction force. When structural vibrations are excited by the microscopic slip events, the generated oscillation of interface stresses and strains in turn affects the local slip dynamics, such that sort of a

synchronized closed-loop dynamics linking both the microscopic slips and the macroscopic vibrations results. In these cases the sliding motion is perceived as intermittent sticking and slipping also on the macroscopic length- and timescale.

In general, when the given sliding velocity is very small, the interface slip events cannot synchronize with structural vibrations, such that the steady sliding results. For intermediate sliding velocities, the appearance of macroscopic stick–slip vs. steady sliding depends strongly on the properties of the interfacial relaxation processes, as well as on the structural vibration properties. The macroscopic stick–slip is then always accompanied by a structural vibration based on at least one structural natural mode. For large sliding velocities separation effects at the interface start to take place and finally lead to vibro-impact type dynamics.

To discuss relevance and limitations of the present results, the present model's generic and specific properties, as well as its fundamental underlying assumptions should be reviewed and contrasted with the results obtained. First of all, geometry and boundary conditions of the model are highly idealized; to a certain extent the real backing plates of a brake pad, and also its countersurface, are compliant; the loading force may not always remain unchanged during braking, the brake pad as a whole is held in position in a compliant fashion, etc. Then, the model is two-dimensional only and it is based on continuum mechanics, and this restriction applies also to the contact interface. It is obvious that the present findings might have limited value for contact zones in which either the number of true asperities is rather low, such that homogenization to continuum mechanics seems implausible, or in which more complicated contact processes (like, e.g. patch formation [17], etc.) are important. Next, the bulk materials have been modeled as isotropically elastic; although this was motivated from the underlying application, most brake pad materials do not come close to isotropic elasticity. Similar comments apply to the friction model, which has simply been taken as velocity-dependent and static; especially for very low relative velocities friction is known to behave dynamically itself, such that time-dependent friction laws should be used [18].

Taking all these idealizations and approximations into account, the model and the computational results do, nevertheless show some generic aspects. First of all, macroscopic sliding is generated or mediated by an ensemble of microscopic relaxational slipping events at the contact interface; the macroscopic motion thus results as spatio-temporal homogenization of the microscopic dynamics. Many previous studies have already suggested this point of view. Beyond this comparatively direct homogenization perspective, the present study does, however, in addition suggest that microscopic interface processes like slip pulses, etc. (on small spatial and short time scales) may also interact with macroscopic structural dynamics (on large spatial and long time scales), through mutual excitation and interaction processes. Intriguingly, the present model and analysis suggests macroscopic stick–slip motion to appear only under such interaction conditions.

What has to be concluded from this discussion? The present study had originated from the need to understand and possibly predict the vibration and noise generation in a friction brake. Taking into account spatial and temporal scales that allow consideration of the dynamic interface processes suggests that in the present configuration stick–slip vibration on the 'macroscopic' length scale can be understood and predicted only on the basis of the underlying interface processes. From the results on the selection of structural vibration modes in stick–slip one might even be tempted to hypothesize that generation or absence of stick–slip can – at least in the present configuration – not be predicted from knowledge about the system on the macro-scale alone. This, of course, would be bad news for the field of friction-induced vibrations in general, since it would be strongly desirable to accomplish modeling, simulation and prediction of friction-affected system dynamics on engineering length scales without having to resort to interface or microscopic considerations as has been done in the present study.

Basically this problem is a matter of separation of scales; most conventional modeling in the low-frequency/large wavelength range rests implicitly on the assumption that dynamic interface processes on underlying high-frequency/small wavelength ranges can be subsumed in some sort of contact and friction law. The present study indicates that there might be cases where the straightforward separation of scales fails and more involved approaches have to be adapted. To further evaluate the relevance of the present findings, however, further studies seem inevitable. Among others, improved material, friction and contact models will have to be considered to improve the representation of the interface dynamics; more realistic geometries and boundary conditions for the bodies involved will have to be considered to understand how, e.g. macroscopic friction self-excitation mechanisms are affected by dynamical interface phenomena; the role of shear and compression waves in the bulk material has to be clarified; it has to be understood why the present study yields slip pulses, and not periodic slip waves; qualitative and quantitative validation based on measurements will be required. The most rewarding objective of such further studies could in fact be an understanding of the conditions under which a separation of scales is possible. It could be hoped that this might then also shed some light on the long-lasting debate on why friction-induced vibrations do even today sometimes seem so hard to predict by modeling and simulation.

## Acknowledgement

Support by Suzlon Wind is gratefully acknowledged.

## References


[1] F. Chen, Automotive disk brake squeal: an overview, *International Journal of Vehicle Design* 51 (2009) 39–72.
[2] N.P. Hoffmann, L. Gaul, Friction Induced Vibrations of Brakes—Research Fields and Activities, SAE 2008-01-2579, 2008.
[3] A. Akay, Acoustics of friction, *Journal of Acoustical Society of America* 111 (2002) 1525–1548.
[4] N.M. Kinkaid, O.M. O'Reilly, P. Papadopoulos, Automotive disc brake squeal, *Journal of Sound and Vibration* 267 (2003) 105–166.
[5] K. Popp, Modelling and control of friction induced vibrations, *Mathematical and Computer Modelling of Dynamical Systems* 11 (2005) 345–369.
[6] H. Hetzler, On moving continua with contacts and sliding friction: modeling, general properties and examples, *International Journal of Solids and Structures* 46 (2009) 2556–2570.
[7] G.G. Adams, Self-excited oscillations of two elastic half-spaces sliding with a constant coefficient of friction, *Journal of Applied Mechanics* 62 (1995) 867–872.
[8] M. Nosonovsky, G.G. Adams, Vibration and stability of frictional sliding of two elastic bodies with a wavy contact interface, *Journal of Applied Mechanics* 71 (2004) 154–161.
[9] K. Ranjith, J.R. Rice, Slip dynamics at an interface between dissimilar materials, *Journal of the Mechanics and Physics of Solids* 49 (2001) 341–361.
[10] S.M. Rubinstein, G. Cohen, J. Fineberg, Detachment fronts and the onset of dynamic friction, *Nature* 430 (2004) 1005–1009.
[11] I. Baillet, V. Linck, S. D'Errico, B. Laulagnet, Y. Berthier, Finite element simulation of dynamic instabilities in frictional sliding contact, *Journal of Tribology* 127 (2005) 652–658.
[12] A. Meziane, S. D'Errico, L. Baillet, B. Laulagnet, Instabilities generated by friction in a pad-disc system during the braking process, *Tribology International* 7 (2007) 1127–1136.
[13] Simulia, Abaqus Theory Manual Version 6.8, 2008.
[14] S. Brunen, S. Hüeber, B. Wohlmuth, Contact dynamics with Lagrange multipliers, *IUTAM Symposium on Computational Methods in Contact Mechanics*, Vol. 3, 2007, pp. 17–32.
[15] R.J. Allemang, The modal assurance criterion—twenty years of use and abuse, *Sound and Vibration* 37 (1) (1983) 36–48.
[16] O.N. Kirillov, A.O. Seyranian, The effect of small internal and external damping on the stability of distributed non-conservative systems, *Journal of Applied Mathematics and Mechanics* 69 (2005) 529–552.
[17] M. Eriksson, S. Jacobson, Tribological surfaces of organic brake pads, *Tribology International* 12 (2000) 817–827.
[18] B. Armstrong-Hlouvry, P. Dupont, C. Canudas De Wit, A survey of models, analysis tools and compensation methods for the control of machines with friction, *Automatica* 30 (1994) 1083–1138.